The electrochemistry of antibody-modified conducting polymer electrodes

Anita Sargent [a], Thomas Loi [b], Susannah Gal [b], Omowunmi A. Sadik [a],*

[a] *Department of Chemistry, State University of New York at Binghamton PO Box 6016, Binghamton, NY 13902-6016, USA*
[b] *Department of Biological Sciences, State University of New York at Binghamton, PO Box 6016, Binghamton, NY 13902-6016, USA*

Abstract

The modification of conducting polymer electrodes with antibodies (i.e. proteins) by means of electrochemical polymerization is a simple step that can be used to develop an immunological sensor. However, the electrochemical processes involved leading to the generation of analytical signals by the sensor have not been fully investigated. In this work, we report on the characterization of the interaction between an antigen, human serum albumin (HSA) and an antibody-immobilized polypyrrole electrode (such as anti-HSA) using cyclic voltammetry (CV) and impedance spectroscopy. This interaction was monitored using electrochemical impedance spectroscopy at three different potentials. The potentials correspond to the three redox states of the electroconducting polymer (i.e. reduced, doped and overoxidized states). Evidence from the CV experiments confirmed that there was a shift in the potential, which was found to be proportional to the concentration. Both the CV and the impedance experiments indicated that this potential-dependent shift could be attributed to antibody–antigen (Ab–Ag) binding. © 1999 Elsevier Science S.A. All rights reserved.

Keywords: Impedance spectroscopy; Antibody–antigen reactions; Cyclic voltammetry; Conducting polymers; Immunochemical sensor

1. Introduction

The number of studies devoted to the use of conducting electroactive polymers (CEPs) as the active components in electrochemical sensors has greatly increased in recent years [1–4]. The main analytical advantage of CEP applications lies in the ability to modify the polymers with different counterions, making them more suitable for the detection of a range of analytes. Previously, we have demonstrated successfully the feasibility of using CEPs for the detection of proteins [5]. In addition, we reported that when conducting polymers and pulsed electrochemical detection (PED) systems were coupled to a flow injection analysis (FIA) system, the combination resulted in a unique approach to obtaining practically useful Ab–Ag signals [5,6]. Subsequently, we reported the development of CEP-based immunosensors for HSA, phenols, phenol derivatives, and thaumatin [6–10]. Despite the very promising analytical signals obtained on these systems, the mechanism by which the CEP enhanced the interaction of Ab and Ag to produce the useful analytical signal had not been fully addressed to date.

The mechanism by which CEPs catalyze Ab–Ag interactions has resulted in some technical challenges due to several reasons. First, the biochemical process often runs in parallel with the charging taking place at the double layer and the mass transport processes at the polymer interface. Secondly, problems arise because of the imprecise description of the state of the interface, the electrical variables, and the concentrations of the reactant and product in the reaction zone. Thirdly, the reaction between Ab and Ag does not involve a redox transfer found typically in the redox transformation of substrate to product at the enzyme-modified CEP electrodes [11–18]. It seems that the mechanism of the Ab–Ag reaction at CEP-based electrodes involves the variation in the capacitive properties of the polymer. Specifically, the interactions between a negatively charged Ab at a neutral pH, plus a delocalized, positive charge along the CEP chain will induce a change in the capacitance of the polymer. This change, resulting in the

* Corresponding author. Fax: + 1-607-777-4478.
E-mail address: osadik@binghamton.edu (O.A. Sadik)

polarization of the electrode, could produce an inherent change in the redox state of the polymer to produce the analytical signal. Changes in capacitance at the electrode | electrolyte interfaces resulting from Ab–Ag recognition at non-conducting polymers have previously been used to develop immunosensors [19,20].

Hence, an excellent knowledge of the underlying mechanism of CEP sensors is required to predict sensor parameters such as the sensitivity, selectivity, and the limit of detection. Generally, such parameters depend on the morphology of the polymer, the bioactivity of the immobilized molecules, and the electropolymerization conditions. Using cyclic voltammetry and impedance spectroscopy, we hereby describe the qualitative picture of Ab-modified CEP electrode during a reaction with an antigen.

1.1. CEP redox chemistry

The presence of a bimolecular component in a CEP film can cause a shift in the redox potential of the film. This redox potential can be used for indirect detection of an antigen. The CEP matrix is able to catalyze the Ab–Ag reaction, resulting in a change in resistance of the polymer as well as an inherent net change in the over-all cell potential. These reactions can be described simply by:

$$E_{overall} = E_{applied} + IR_{solutions} \tag{1}$$

Previous workers have shown that CEPs display both capacitive and faradaic charges observed in the high steady state currents of their cyclic voltammetry (CV) [21,22]. From the CV, the authors also reported that the corresponding capacitance of the CEPs was as high as 100 F g^{-1} [23]. Yet, other workers claimed that these two-component charges could be evaluated using impedance analysis [24,25]. Theoretical evidence by other workers indicated that these two charges could not be separated [26]. Some suggested an alternative approach of explaining these based on the determination of the n and $E°$ values from the charge–potential curve [27]. However, since the charge–potential relationship must be obtained at equilibrium conditions, its determination from the CEPs point of view is usually accompanied by hysteresis. Generally, this phenomenon could be attributed to an asymmetric structural change, particularly in the process of 'swelling' or 'deswelling' of the polymer [27]. Since the polymer was modified with an antibody in our own study, the robust electrochemical properties of the conducting polypyrrole employed did necessarily 'override' the small, selective signal arising from the Ab–Ag binding event. Consequently, we used the ac impedance technique to study the resistivity instead of the conductivity. This choice was due to the binding event being characterized by a change in the double layer capacitance, (C_{dl}) and the charge transfer resistance as a function of frequency, among other obtainable variables.

2. Model of Ab–Ag interactions at the CEP interface

In order to correlate CEP processes with Ab–Ag interactions, we present a two-dimensional surface model involving the binding of HSA to an electrochemically oxidized polypyrrole surface. This model involves the diffuse layer of the charge in the solution such as shown in Fig. 1. The antibody-immobilized polypyrrole film (PPy–AHSA) has two interfaces consisting of a platinum | polypyrrole interface (Pt | PPy), and a polypyrrole | solution interface (PPy | solution). Electron exchange occurs between the Pt | PPy interface while only ion exchange takes place at the PPy | solution interface. Thus, the adsorption of protein with n number of molecules at the PPy | solution interface will change the amount of charge at the electrical double layer. This means that the greatest concentration of excess charges is adjacent to the PPy | solution interface, where electrostatic forces are most able to overcome the other processes involved. Therefore, a progressively smaller concentration can be observed at the furthest distances away from the interface as those forces become weakened. Hence, the average distance will be dependent on the applied potential, the pH and the analyte concentrations. If the sensor is poised at an oxidizing potential, the Ab–Ag interaction will be enhanced as the solvation spheres meet. This implies that the capacitance will decrease as the two highly charged molecules interact. Concurrent with this process is a rise in the exchange current, signifying the transport of these charges throughout the bulk of the polymer.

On the other hand, the interaction may be discouraged when the potential is stepped back to a reducing value as depicted in Fig. 1 [6,10]. During this process, the capacitance increases back to its original value prior to Ab–Ag complexation. The interactions between the immobilized AHSA (pI = 4.7), which are mainly negatively charged at neutral pH, and the delocalized positive charges along the polymer chains both help to induce changes in the capacitance of the material. These interactions are evident from the electrochemical measurements and they form the basis of the bioaffinity signals. This paper shows that the variation in the capacitive currents at the polymer | protein interfaces obeys the mechanistic model described.

3. Experimental

3.1. Reagents

All solutions were made up in Nanopure deionized distilled water (17.5 MΩ cm) unless otherwise stated. Anti-human serum albumin (AHSA), made up of 59 mg ml^{-1} total protein, and 4 mg ml^{-1} specific antibody, was purchased from Sigma (A-7544). This was dialyzed

against phosphate buffer (PBS) of pH 7.2 before being frozen and stored in working aliquots. NaCl (99%) was purchased from Aldrich Chemicals and stored in a desiccator. The HSA used was also purchased from Sigma (A-1887) and stored at 4°C, while pyrrole was also obtained from Aldrich Chemicals and distilled before use. All references to PBS are at a pH of 7.2.

3.2. Instrumentation

The electrochemical instrumentation used in these experiments consisted of an EG&G potentiostat/galvanostat (Model 263A) and EG&G lock-in-amplifier (Model 5210). All data collection and analysis were conducted using electrochemistry software Model 270 and electrochemical impedance spectroscopy (EIS) software Model 398. The EG&G model 5210 lock-in amplifier was used to generate frequencies above the 10 Hz levels, while the EG&G potentiostat Model 263A was used to control the potential and to generate frequencies below 10 Hz levels. Each impedance spectrum was recorded at two different wave ranges. These include a single sine wave in the range 100 kHz to 15.85 Hz and a multi-sine wave measurement in the remaining lower frequencies ranging from 10 Hz to 88.46 mHz. These two frequency ranges were combined together with the 'autoexecute' option available on the EIS software EIS M398 so that the experiment could cover the entire range of frequencies. The experiments were conducted using a three-electrode cell, consisting of a BAS platinum-disc working electrode (area = 0.0201 cm^2), an aqueous Ag | AgCl | KCl(sat) as the reference electrode and a platinum wire as the auxiliary electrode.

3.3. Experimental

Polymers were prepared by galvanostatic polymerization using a current density of 0.3 mA cm^{-2} from a 10 ml PBS solution. The PPy–PBS was prepared using 0.5 M pyrrole with the PBS as the supporting electrolyte. Also, the PPy–AHSA films were prepared in a solution containing 0.5 M pyrrole with anti-HSA 0.59 mg ml^{-1} of the total protein in the PBS. The overoxidized PPy was prepared using the same composition as in PPy–AHSA, and this was cycled for a considerable period in the buffer. All measurements were taken using 10 ml PBS (pH 7.2) purged with N_2 for 10 min and then blanketed for the remainder of the experiment. All freshly grown polymer films were characterized using cyclic voltammetry (CV) at a scan rate of 50 mV s^{-1} in 0.1 M NaCl (unless otherwise stated). The charge passed during polymerization for PPy–PBS was 16.5 mC, while that for PPy–AHSA was 8.0 mC.

The PPy–PBS films were subjected to the same analysis conditions specified for the Ab-containing electrodes, and used as the control. The PPy–AHSA films were first characterized in 0.1 M NaCl and then incubated in 0.1% BSA at room temperature for
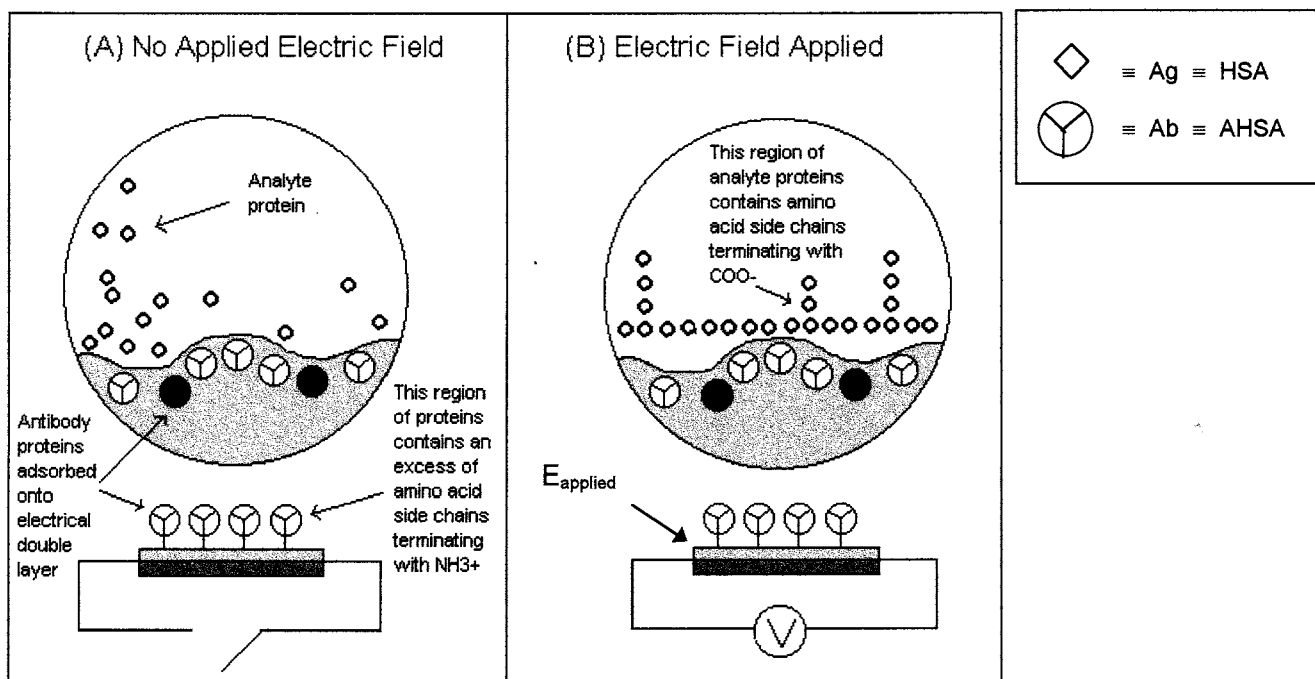

Fig. 1. (A) Proposed model of the antibody-immobilized polymer | solution interface; (B) Schematic of pulse-modulated Ab–Ag interactions (arrow indicates that the potential was applied across the interface).
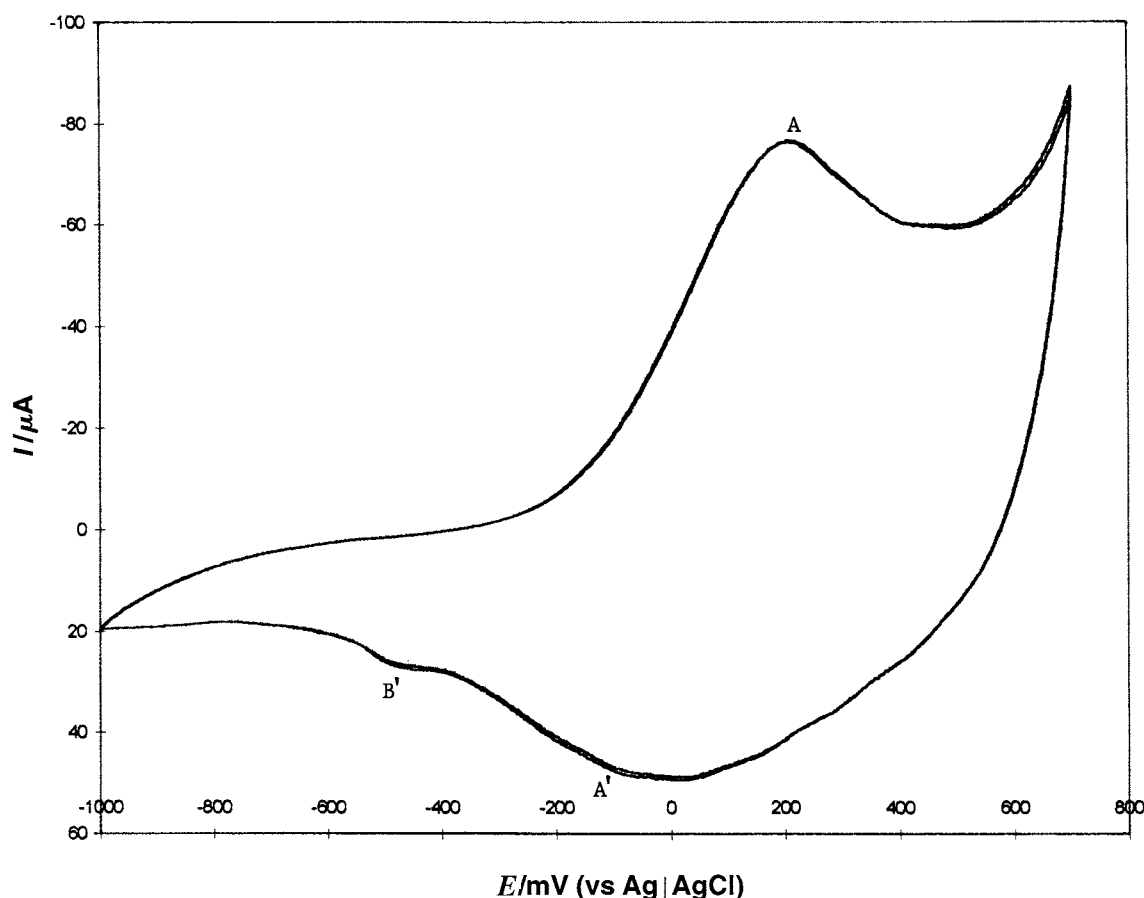
Fig. 2. Cyclic voltammogram obtained for antibody-immobilized polymer electrode. Scan rate = 50 mV s^{-1}, supporting electrolyte = PBS buffer at pH 7.2.

about 30 min in the presence of PBS solution to eliminate nonspecific adsorption. The impedance analysis of the films was carried out using PBS solution in the presence of 100 μg ml^{-1} HSA. As for the AHSA containing the over-oxidized films, the AHSA–HSA complexation within the film was accomplished by incubating the PPy–AHSA film in PBS in a solution of 100 μg ml^{-1} HSA. This was left overnight at 4°C for about 20 h. For the over-oxidized PPy–AHSA films, the impedance spectra of each film were recorded at bias voltages of -0.6, -0.4, -0.2, 0, 0.2 and 0.4 V, respectively using a frequency range of 100 kHz to 88.46 mHz. For the electroactive PPy–AHSA films at an amplitude of 15 mV, the frequency range was between 100 kHz and 10 mHz. Impedance parameters such as the uncompensated ohmic resistance, (R_s), charge transfer resistance (R_{ct}), and the angle of depression (θ), were extracted from the semicircle points of the Nyquist plots. In several instances, a small, but high frequency semicircle was followed by a much larger (incomplete) semicircle. In such cases, valuable parameters were extracted from the high-frequency data only. The value of the double-layer capacitance (C_{dl}) was determined using the intercept (i.e. at $\omega = 1$ rad s^{-1}) of

the Bode plot. In many cases, the Bode plot revealed clearly two separate time constants, and all data extracted were taken from the first set of time constants (i.e. those at higher frequencies).

4. Results and discussion

4.1. Characterization of antibody-immobilized polymer films using cyclic voltammetry

Part of the focus of this study was to investigate how a change in the voltammetric behavior of an Ab–immobilized PPy membrane in a buffer medium could be used to probe Ab–Ag interaction. Polymers were synthesized as described in Experimental. The supporting electrolyte used in all of the experiments was phosphate buffer (pH 7.2) unless otherwise stated. Fig. 2 shows the typical behavior of PPy electrodes in PBS buffer. The figure indicates that when the potential was scanned between -1.0 to $+0.6$ V, one pair of peaks was observed together with an extra peak on the reverse sweep. The first pair (A/A′) was located at about $+0.1$ V. The extra peak labelled as B′ located on the reverse

sweep was at -0.5 V. This type of behavior was similar to that observed during previously reported data for PPy–DS films [13,14]. Therefore, the voltammetric behavior suggests that the mechanism of the redox process may involve both cation and anion exchange at the electrodes.

4.1.1. Effect of antigen concentration

The voltammetric behavior of PPy–AHSA using varying concentrations of antigen at PPY–AHSA was

studied. When no antigen was present, the CV for the Ab–containing PPy electrode was reduced from $+1$ to 0 state at a cathodic peak potential (E_{pc}) of 0.0 V versus the Ag $|$ AgCl reference electrode as shown in Fig. 3A. The separation between the anodic and cathodic peak potentials (ΔE_p) of 0.20 V indicated a quasi-reversible electron transfer process that was maintained in the presence of the antigen together with an apparent shift in the $E_{1/2}$. The $E_{1/2}$, (i.e. the average of E_{pc} and $E_{pa'}$) was estimated to be 0.10 V in the absence of the
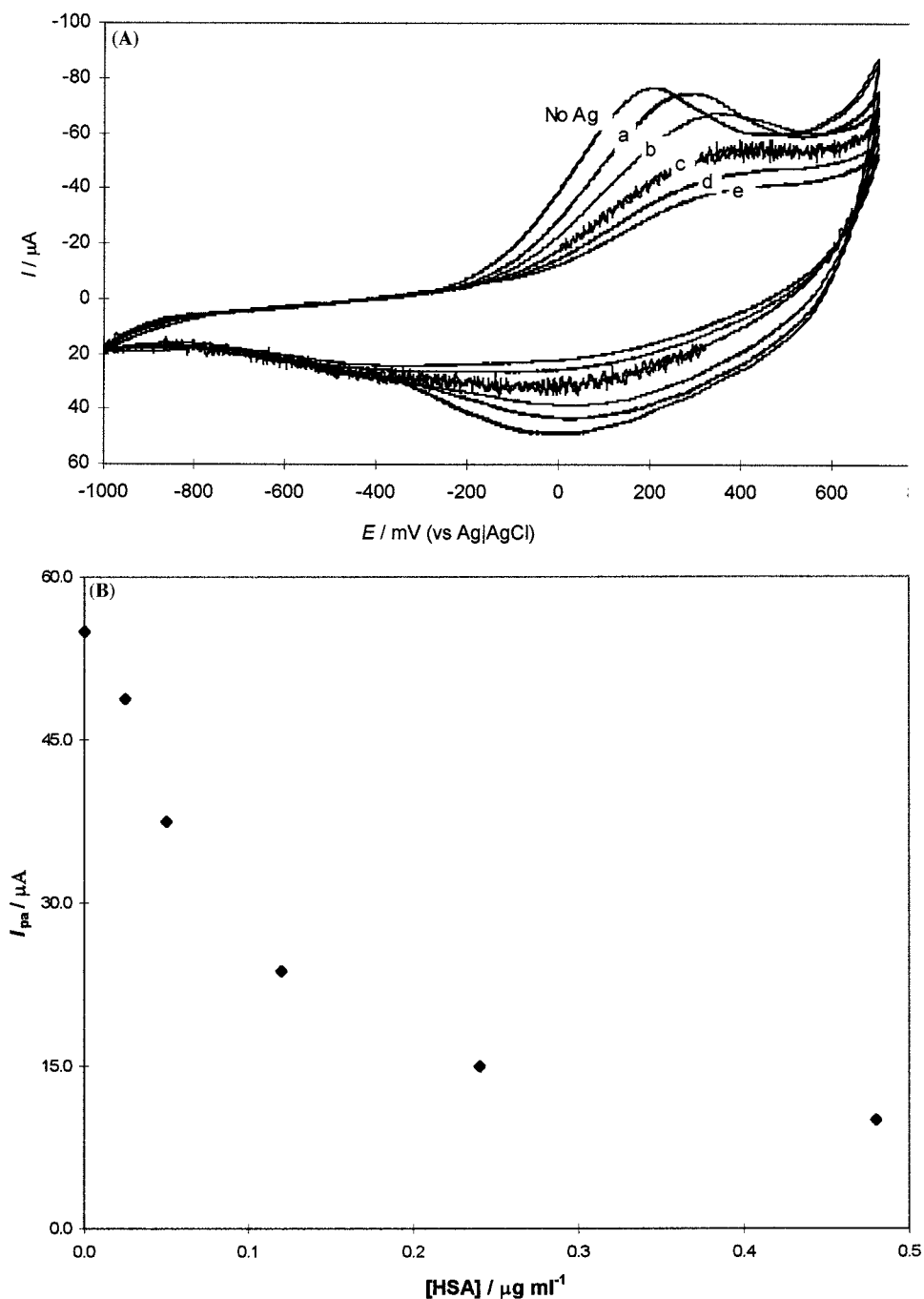

Fig. 3. (A) Voltammogram obtained at different antigen concentrations; (—) No antigen; (a) 0.025 µg l^{-1}; (b) 0.05 µg l^{-1}; (c) 0.12 µg l^{-1}; (d) 0.24 µg l^{-1}; (e) 0.48 µg l^{-1}. (B) Plot of anodic current versus concentration. Other conditions as in Fig. 2.
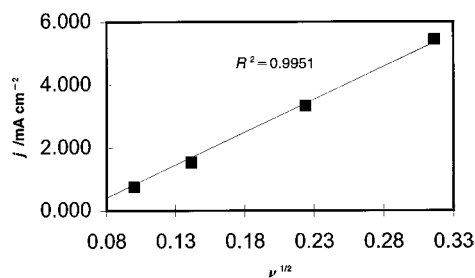
Fig. 4. Dependence of anodic peak current as a function of the square root of scan rates at the PPy|AHSA electrode, supporting electrolyte = PBS buffer at pH 7.2.

antigen. Also, in the presence of 0.025 µg ml^{-1} antigen, the E_{pc} and E_{pa} were 0.06 and 0.20 V, respectively. Thus, both of the anodic and cathodic peak potentials shifted to more positive values, unlike the solution without antigen. The positive shift in $E_{1/2}$ with increasing antigen concentrations indicated that the oxidation of the PPy film was coupled to a kinetic process, which in this case was the binding of the antigen. This was further evidenced from the CV response, changing from a diffusion-controlled mode (ie. definite peaks in the absence of antigen) to kinetic-control (i.e. the disappearance of peaks and the formation of a plateau) as the antigen concentration increased. This observation suggested a difference in the binding properties of the oxidized and reduced PPy–antibody electrodes and the antigen (Fig. 3).

In addition to changes observed in $E_{1/2}$ upon addition of antigen, there was a corresponding decrease in the CV currents with increase in the antigen concentration (Fig. 3B). In addition, the plots of the cathodic peak current (I_{pc}) versus $v^{1/2}$ in Fig. 4 were linear, having an intercept close to zero as expected for reversible electron transfer. We attributed this change in current (after adding Ag) to the difference in the equilibrium mixture of the free and bound species to the electrode surface. Thus, the decrease in current observed in the CV experiments could be attributed to the binding of the PPy–AHSA to a large, slowly diffusing HSA molecule and an inherent impediment in polymer redox activity. The linearity of the peak current versus the square root of the scan rate, as well as the linear dependence of the peak potentials with scan rate, indi-

cated a diffusion-controlled response. These could be the result of the contributions from the charge transport within the electroactive polymer.

In order to ascertain the response to diffusion of the solution species, attempts were made to show that the charge transport within the film was fast enough, but not rate limiting. However, the diffusion coefficient for the HSA could not be determined directly from the CVs. Nevertheless, the diffusion at PPy films depended on sufficient uptake and expulsion of ions from the solution. With the presence of HSA, the majority of the diffusion would be due to the relatively smaller ions in the solution. Consequently, HSA would bind to Ab-immobilized PPy, but due to its large size and folded nature, it was incapable of diffusing within the PPy matrix to produce a measurable change in the conductivity. Hence, as the antigen formed a complex with the immobilized antibody, the diffusion of the smaller ions would be hindered through the blocking of their pathways into the conducting polymer. Inherently, this resulted in a decrease in current with the concentration of HSA as shown in Fig. 3B.

4.1.2. Proposed mechanism of ion-exchange at CEP-modified antibody electrodes

The mechanism of the interaction at PPy-antibody electrodes can be explained as follows: when the polymer is switched between +1 and 0 oxidation states, charge transport occurs between the antibody and the electrode. Thus, the antibody functions as a polymer 'dopant'. Unlike ordinary dopant, the incorporated antibody is scarcely undoped or released even when reducing the PPy|Ab electrode at −1.00 V versus Ag|AgCl. Undoping the 'dopant' antibody in the polypyrrole signifies a tight network of specific, composite structure of 'twining antibodies' with the PPy matrix. The charge balance is kept by incorporating cations (or supporting electrolyte) into the reduced PPy–Ab as counterion. This can be depicted as shown in Scheme 1.

From this mechanism, we could infer that there was no desorption of the large AHSA macromolecules when the polymer was reduced in the first redox cycles. Instead, the insertion of Na$^+$ cation into the electrolyte helped in the formation of the PPy$^+$–AHSA–Na$^+$
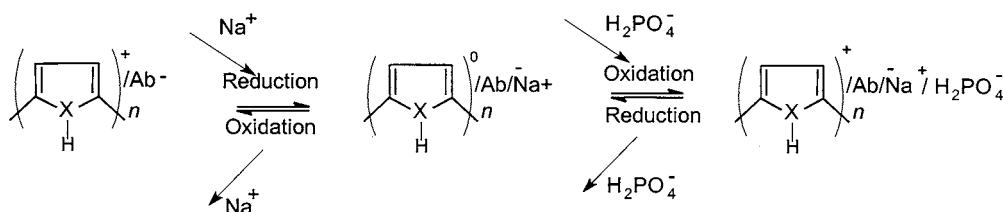
Scheme 1. Mechanism of Ion exchange at CEP-modified antibody electrodes. The antibody is negatively charged with an isoelectric point of 4.7 at neutral pH.

complex. The anodic and cathodic waves could therefore be explained using cation insertion. The cation inserted in the polymer matrix would interact with the negatively charged AHSA counterion, as shown in Scheme 1. This mechanism is consistent with the voltammetric data obtained at a PPy–AHSA electrode. The current magnitudes for the first pair of peaks increased linearly with the scan rates. This also is in line with the characteristic of electroactive species on electrode surface.

4.2. Impedance spectroscopy of antibody-containing polypyrrole electrodes

Some workers have shown that polypyrrole acts as an insulator at negative potentials [17]. This means that dopant anions are expelled into the solution phase, leaving the polymer in its neutral, non-conductive state. When the potential is sufficiently negative, e.g. at -0.6 V, a kinetically controlled electrode process becomes dominant. However, at positive potentials, the PPy changes electrochemically to its conductive state, thus allowing the diffusion of the anions (dopants) into the film. This anionic uptake is responsible for the polymer exhibiting its desirable electrochemical properties. Again, at positive potentials, we believe that diffusion plays an obvious role in the electrode process. Consequently, we examined the electrochemistry of Ab-containing CEP electrodes further using impedance spectroscopy. The impedance was studied at three different redox states of the electroconducting polymer, including the reduced, doped and overoxidized states.

4.2.1. Charge-transfer processes at PPy–PBS electrode

The charge transfer processes at a polypyrrole electrode containing no immobilized antibody was first studied. This control experiment utilized polypyrrole prepared by using the buffer solution (i.e. PPy–PBS). PPy–PBS electrode was used as the blank polymer under similar experimental conditions as the sensing electrodes and the effect of applied potential was investigated. When the potentials became sufficiently negative, e.g. from -0.6 and -0.4 V, the polymer existed largely in its reduced form. Hence, the charge transfer of the PPy–PBS film was very limited due to kinetic control as shown in Fig. 5a. Presumably, the reaction should slow down at this potential due to the switching from an oxidized to a neutral form. In the oxidized form, i.e. at potentials ≥ -0.2 V, there was a distinction between the semi-infinite and finite-length diffusion behavior observed through the characteristic curve. In addition, the 'complex plane' impedance curve revealed a deviation from the depressed semicircle (at negative potentials) towards a limiting real impedance behavior (at positive potentials).

Moreover, at -0.4 V, the electrode process changed from kinetic control at high frequency to diffusion control. At this point, the Nyquist slope was 1 and Z'

ranged from 2 to 5 kΩ. Fig. 5b is an enlargement of Fig. 5a at a higher frequency region and at all potentials. This figure shows that the Nyquist plot switched from diffusion (or kinetic control) to saturation as indicated by the vertical curves in the figure, where the Nyquist slope approached infinity. In addition, the capacitance at the switching frequency was a measure of the charge storage capacity of the polymer at the given potential. This implied that at positive potentials, the charge-transfer process was rapid and reversible, and this occurred within the finite region where the PPy–PBS acted as an infinite capacitor. Table 1 illustrates this tendency toward high capacitance at positive potentials and is synonymous with previous observation when the PPy electrode was doped with small molecular weight anions [16,17,28]. Beyond -0.4 V level, the charge transfer resistance became very negligible. Thus, it was no longer feasible to calculate I_o from the impedance data. The voltammograms recorded for PPy–PBS (before and after the impedance analysis) revealed that the electrochemical properties of the film were not compromised significantly by the EIS as shown in Fig. 6. Table 1 is a summary of the electrochemical parameters obtained from the impedance spectra for all PPy films investigated.

4.2.2. Charge-transfer processes at PPy–AHSA electrode

Using an Ab–containing PPy electrode, we studied the effect of applied potential on charge-transfer. Fig. 7 shows the Nyquist plots of PPy–AHSA in PBS and PPy–AHSA in HSA–containing solutions. Fig. 7(a) shows the plots obtained for PPy–AHSA in PBS at the potential region between -0.6 and 0.4 V. These spectra showed that there was a switch from kinetic-controlled behavior to diffusion controlled characteristics at lower frequencies. In contrast with the PPy–PBS film, this phenomenon was synonymous to an infinite capacitor at low frequencies. Since the ions are small-sized, and diffused easily through PPy–PBS films, there was no measurable charge-transfer resistance at higher potentials.

At positive potentials, a higher charge–transfer resistance existed in the PPy–AHSA film relative to the PPy–PBS film. Table 1 provides a summary of these observations. From this table, we could infer that the high charge transfer resistance was probably due to the inability of the entrapped biomolecules to diffuse within the film. At low values of Z' (i.e. 0 and 4 kΩ), the Nyquist plot was characterized by semi circles, indicating that the system was kinetically controlled. At intermediate Z' values (i.e. 4–25 kΩ), the PPy–AHSA electrode began to switch from a kinetic controlled, limited process to a diffusion limited process where the electrode potential changed from -0.6 to 0.4 V (data not shown). Fig. 7b is the Nyquist plot obtained for PPy–AHSA when exposed to HSA solution. When the PPy–AHSA polymer was exposed to HSA solution,

Table 1
Summary of impedance spectroscopy data using antibody-containing CEP films

	Bare Pt *						PPy-PBS					
Bias/mV	-600 [a]	-400	-200 [a]	0 [a]	200 [b]	400 [a]	-600	-400 [a]	-200 [c]	0 [c]	200 [c]	400 [c]
R_s/Ω	301	300	303	303	302	245	434	382	N/A	N/A	N/A	N/A
R_{ct}/Ω	562	2149	10797	10177	15958	92546	93706	1260	N/A	N/A	N/A	N/A
$C_{dl}/\mu F$	30.8	16.8	16.4	17.7	12.3	9.0	14.3	121	680	1229	1484	1499
$j_o/\mu A\ cm^{-2}$	2274.9	594.6	118.3	125.5	80.1	13.8	13.6	1014.3	N/A	N/A	N/A	N/A
θ	-16.7	-20.5	-14	-14.2	-15.3	-23.9	-43.3	-24.5	N/A	N/A	N/A	N/A
	PPy-AHSA						**PPy-AHSA in HAS**					
Bias/mV	-600	-400 [b]	-200	0 [b]	200 [b]	400 [b]	-600 [b]	-400	-200	0	200	400
R_s/Ω	726	325	257	245	238	231	331	381	263	253	248	245
R_{ct}/Ω	48714	7620	2105	1056	914	862	19800	10910	1330	730	890	870
$C_{dl}/\mu F$	5.4	14.9	93.7	213	301	331	5.5	11.6	87.6	210	182	155
$j_o/\mu A\ cm^{-2}$	26	168	607	1210	1399	1482	65	117	962	1762	1435	1460
θ	-34.5	-28.5	-31.4	-32.1	-34.1	-36.2	-21.1	-25.1	-23.6	-24.9	-28.6	-27.5
	Overoxidized PPy-AHSA						**Overoxidized PPy-AHSA-HSA**					
Bias/mV	-600	-400 [a]	-200 [a]	0 [a]	200 [a]	400 [a]	-600	-400 [a]	-200 [a]	0 [a]	200	400
R_s/Ω	441	422	413	411	440	465	579	535	518	522	510	559
R_{ct}/Ω	25649	2707	1514	1055	1550	3018	716021	84165	57512	68488	182590	310541
$C_{dl}/\mu F$	27.7	34.3	81.6	205	124	53.3	25.0	4.4	6.3	5.1	5.4	4.8
$j_o/mA\ cm^{-2}$	49.8	472.0	844.1	1210.8	824.3	423.4	1.8	15.2	22.2	18.7	7.0	4.1
θ	-40.7	-10.4	-14.6	-22.7	-20.8	-22.6	-28.4	-12.4	-13.7	-16.3	-16.7	-13.8

[a] Diffusion controllod behavior observed in Nyquist plot.

[b] Two overlapping semi-circles observed; highest frequency fit used for calculations.

[c] Diffusion-controlled behavior throughout most of frequency range.

* On bare Pt, R_{ct}, increases while C_{dl}, decreases at more anodic potentials; this behavior is in contrast to all PPy films examined. This confirms that PPy acts as an infinite capacitor at anodic potentials.
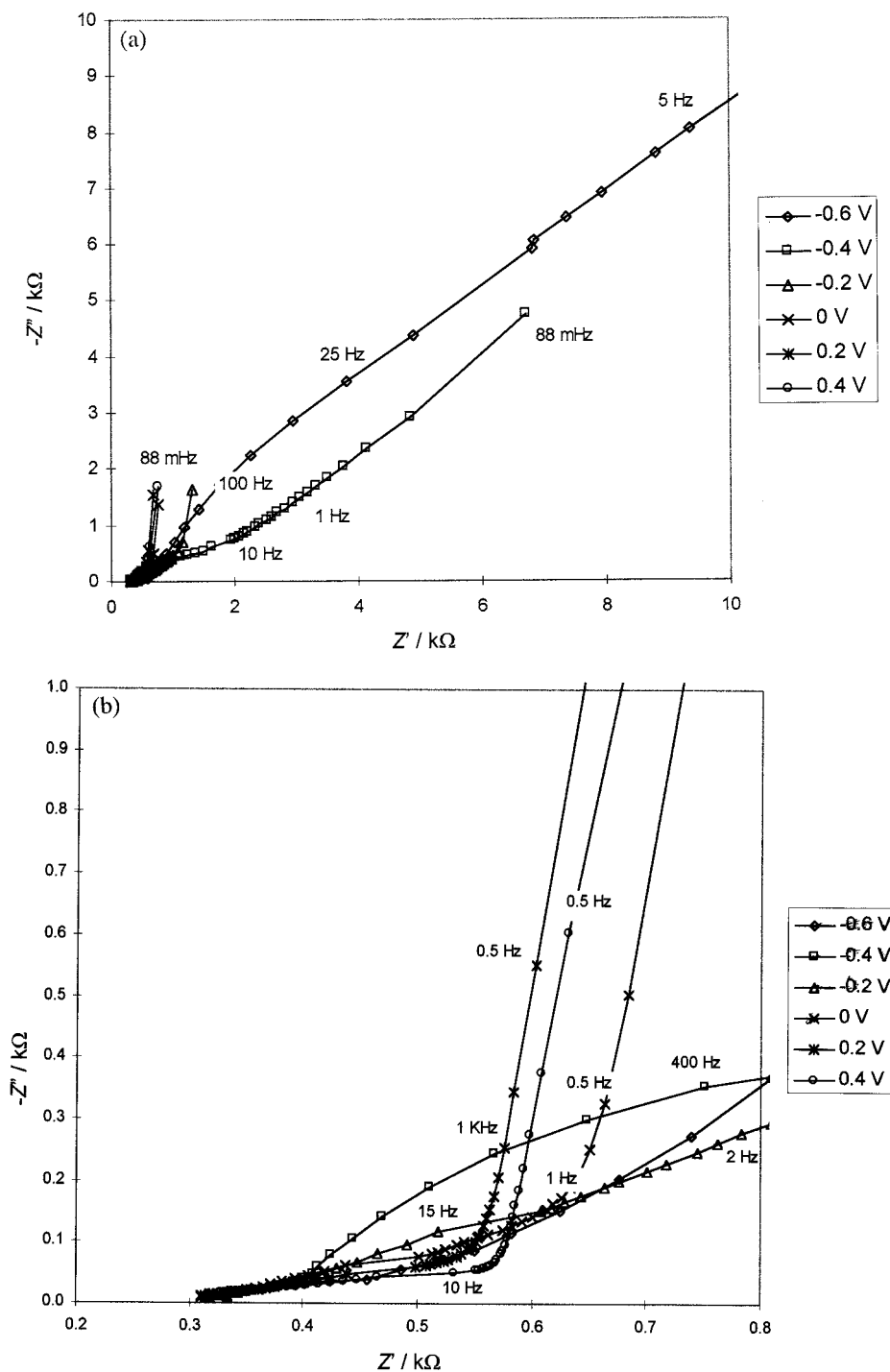
Fig. 5. (a) Nyquist plot of PPy–PBS film in PBS, pH 7.2 at −0.6 and −0.4 V; (b) Nyquist plot of PPy–PBS film in PBS at all potentials. Conditions are as in (a).

slightly lower charge-transfer resistance was observed at potentials above −0.2 V. This is expected since the electrode became increasingly electroactive as the potential moved toward positive values. Therefore, the reactivity of the electrode depended on the diffusion of the charges within the polymer. The presence of two kinetically controlled regions at negative potentials may be attributed to PBS desorption and cation insertion

into the PPy as depicted in Scheme 1. This observation is consistent with the proposed mechanism.

Fig. 8 shows the double-layer capacitance of the PPy–AHSA as a function of applied potential, indicating that the capacitance increased gradually when the polymer was oxidized, although not to the same extent as the blank polymer (PPy–PBS). This result supports previous reports of capacitance changes observed at a
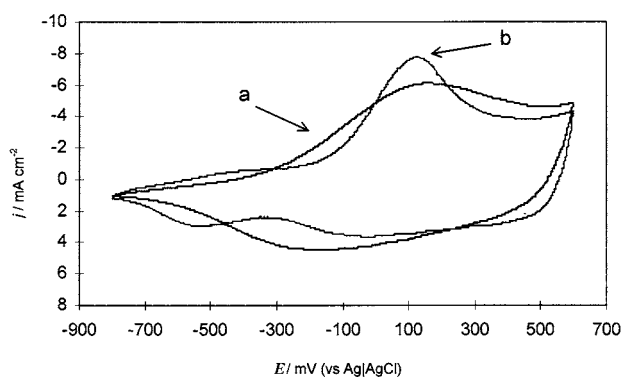
Fig. 6. CV of PPy/PBS film in 0.1 M NaCl (a) before and (b) after impedance measurements in PBS; scan rate = 50 mV s^{-1}.

non-conducting polymer [29,30]. In those studies, Ab–Ag interactions were reported to produce capacitance changes of about 50 000 pF cm^{-2} with a maximum standard deviation of about 30 pF cm^{-2} using an electrode size of 0.3 cm^{-2} [29,30]. Since the present study utilized CEPs, the redox contribution from the CEP backbone should affect the capacitance significantly. Our results produced a large capacitance change of about 30 μF for an electrode size of 0.0201 cm^2 and a standard deviation of 0.02 μF cm^{-2}. The larger capacitance measured could be attributed to a contribution from the CEP matrix during the Ab–Ag processes.

From Fig. 8, it can be seen that the capacitance of PPy–AHSA interacting with HSA in solution decreased immediately with increasing potentials from 0 V and above. Beyond certain positive potentials, the exchange
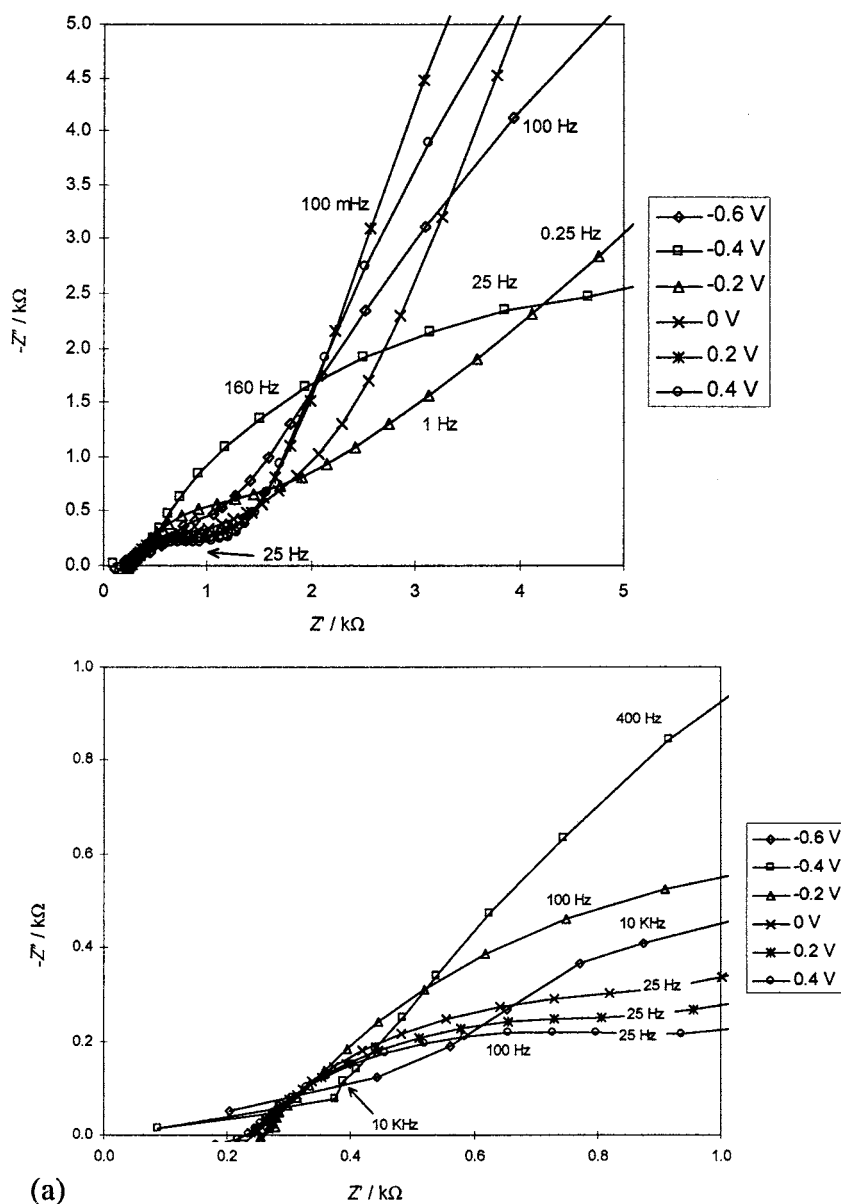

(a)

Fig. 7. (a) Nyquist plots of PPy–AHSA in PBS; (b) Nyquist plots of PPy–AHSA in 100 μg ml^{-1} HSA in PBS.
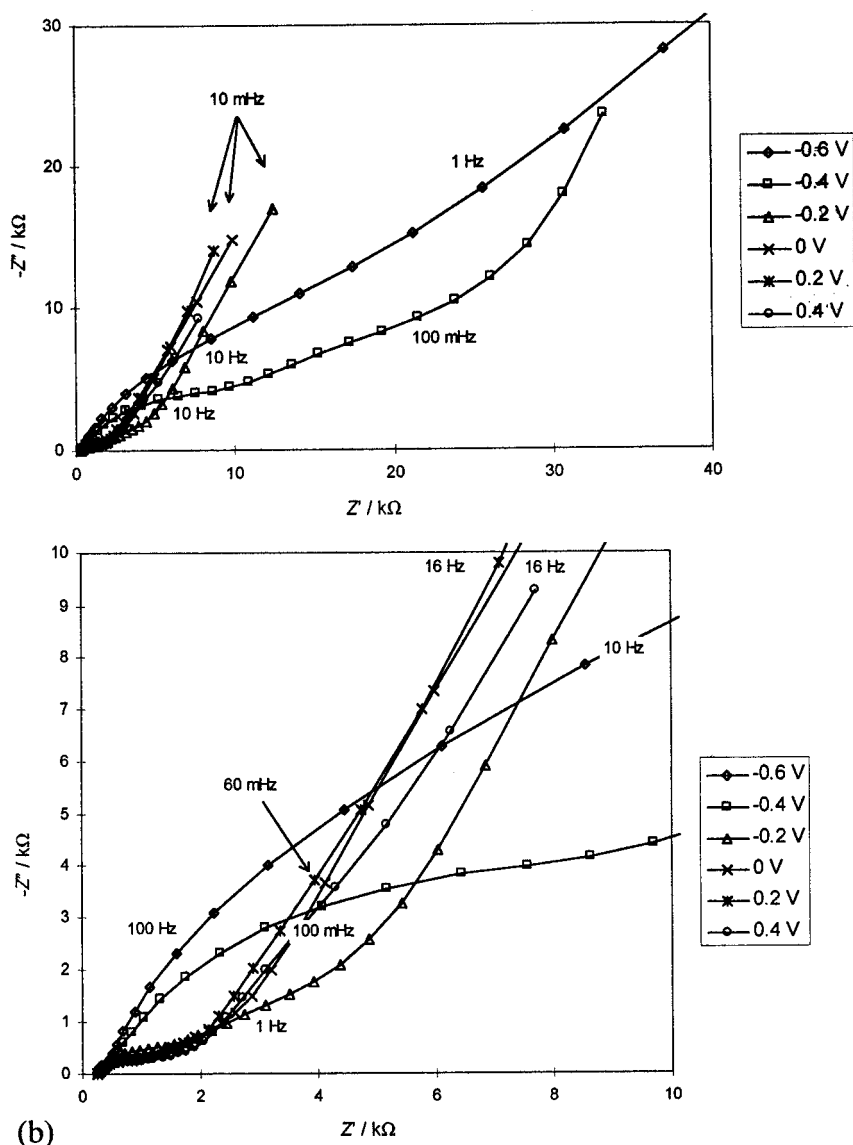
Fig. 7. (Continued)

current returned to its normal pathway as indicated in Table 1. However, C_{dl} remained low at these positive potentials because Ag was still bound to the Ab at the electrode surface, thus maintaining the charged interaction. This very much agreed with the mechanism of ion exchange at CEP outlined earlier. As more thresholds of available binding sites in the polymer matrix occurred, R_{ct} and I_o levelled off at the optimum binding potentials (Table 1). The CV of the film recorded in the presence of HSA revealed that the electroactivity of the PPy–AHSA film became suppressed in the HSA solution. This was consistent with the earlier explanation for Ab–Ag reaction. Hence, blocking the pathways into the conducting polymer could hinder the diffusion of smaller ions, resulting in the suppression of polymer activity as confirmed from the CV recorded afterwards (Fig. 9).

4.2.3. Charge-transfer processes at over-oxidized PPy–AHSA electrode

The stability of the polymer material to 'potential cycling' can be used to predict its response to the analytes. We studied the effects of charge transfer dynamics at over-oxidized PPy–AHSA film. Using CV, we confirmed that over-oxidation of the film occurred, through a loss in the electroactivity of the film. The over-oxidized PPy–AHSA film was then exposed to corresponding antigen (HSA). Fig. 10 indicates that kinetic control was most apparent and no diffusion behavior was observed. This was expected since little or no significant diffusion within the HSA-bound AHSA film should occur. Upon formation of AHSA–HSA complex, the double layer capacitance decreased significantly when the potential became higher than -0.6 V (also confirmed from Fig. 8). This decrease in capaci-
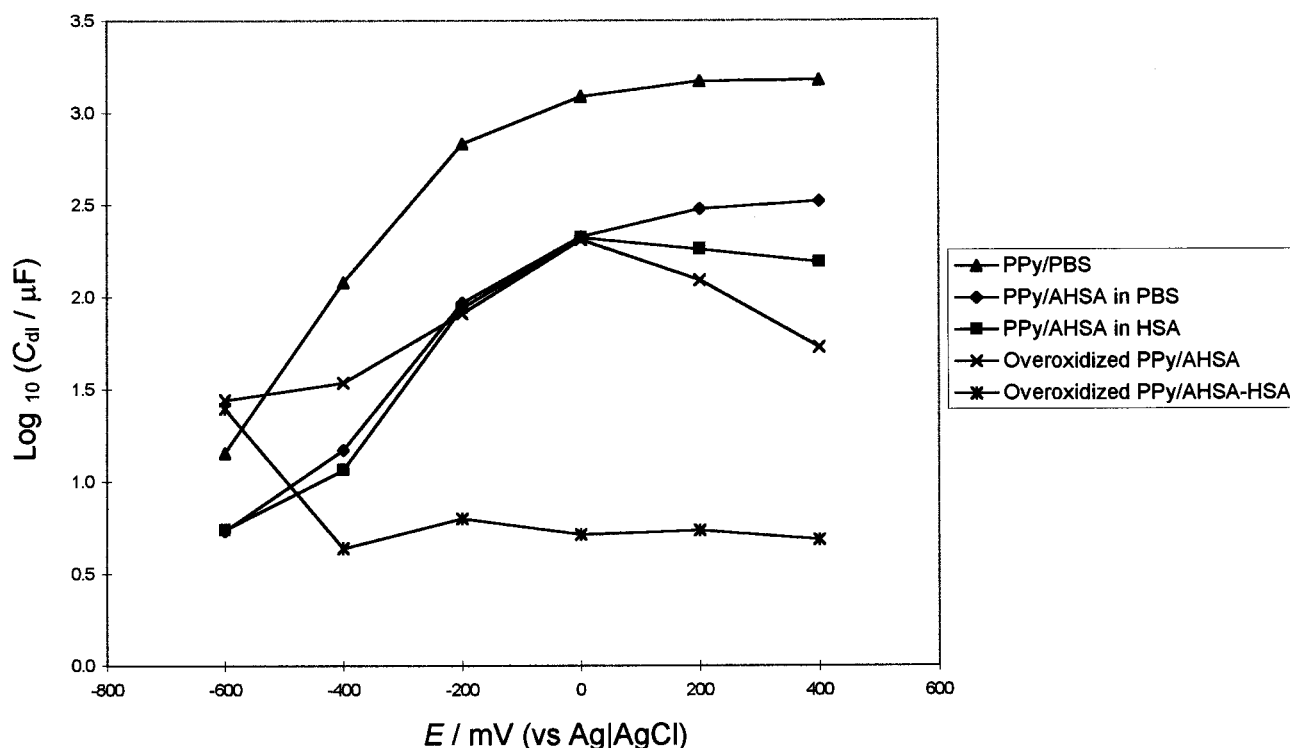
Fig. 8. Plot of log C_{dl} versus potential for all films studied. Other conditions as in Fig. 5.

tance was expected since the long, incubation time with antigen allowed Ab–Ag complexes to form at equilibrium.

In addition, as expected, the presence of AHSA in the over-oxidized polymer film introduced a considerable charge transfer resistance. At negative potential, e.g. -0.6 V, the over-oxidized PPy–AHSA film had a higher charge transfer resistance than the PBS-incorporated film as shown in [1] [11]. This meant that at -0.6 V, charge transfer occurred more readily in the over-oxidized PPy–AHSA film than in the PPy–PBS, although one would expect the polymer conductivity to be somewhat compromised in the presence of huge biomolecules. Nevertheless, diffusion-controlled behavior was still observed in this film. The minimum R_{ct} for the over-oxidized PPy–AHSA–HSA occurred at -0.2 V versus Ag | AgCl at 57512 Ω as shown in Table 1. At this potential, the PPy–AHSA film exhibited the maximum j_o (22 μA cm^{-2}). At higher potentials, the exchange current density decreased, revealing a nearly symmetrical shape right about the maximum. This behavior was associated with overoxidation of the polymer matrix.

5. Conclusions

The electrochemistry of antibody-immobilized CEP electrodes were studied using cyclic voltammetry and impedance spectroscopy techniques. The CV experi-

ments indicated a shift in potential, which was found to be proportional to antigen concentration. Impedance measurements using the antibody-modified electrode showed that larger values of C_{dl} were observed at higher positive potentials with a transition from kinetic control to a diffusion control. At approximately -0.2V, a very abrupt and dramatic jump in C_{dl} accompanied this transition. This increase in C_{dl} with increasing potential was attributed to changes in the structure of the interface associated with the introduction of the first cationic sites into the film. However, beyond 0 V, a decrease in C_{dl} values was observed for the antibody-immobilized polypyrrole electrodes upon exposure to HSA solution
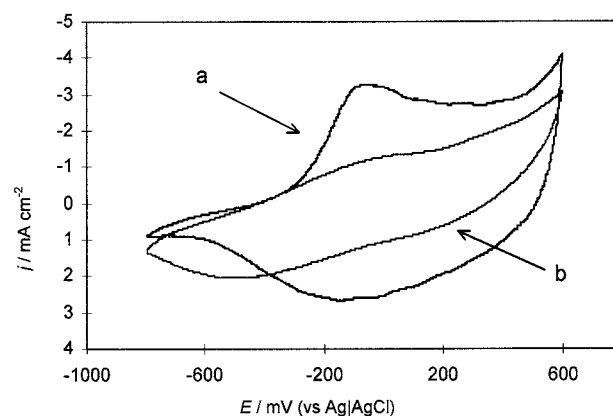

Fig. 9. PPy–AHSA (a) before and (b) after impedance in 100 μg ml^{-1} HSA in PBS. Supporting electrolyte = 0.1 M NaCl; scan rate = 50 mV s^{-1}.
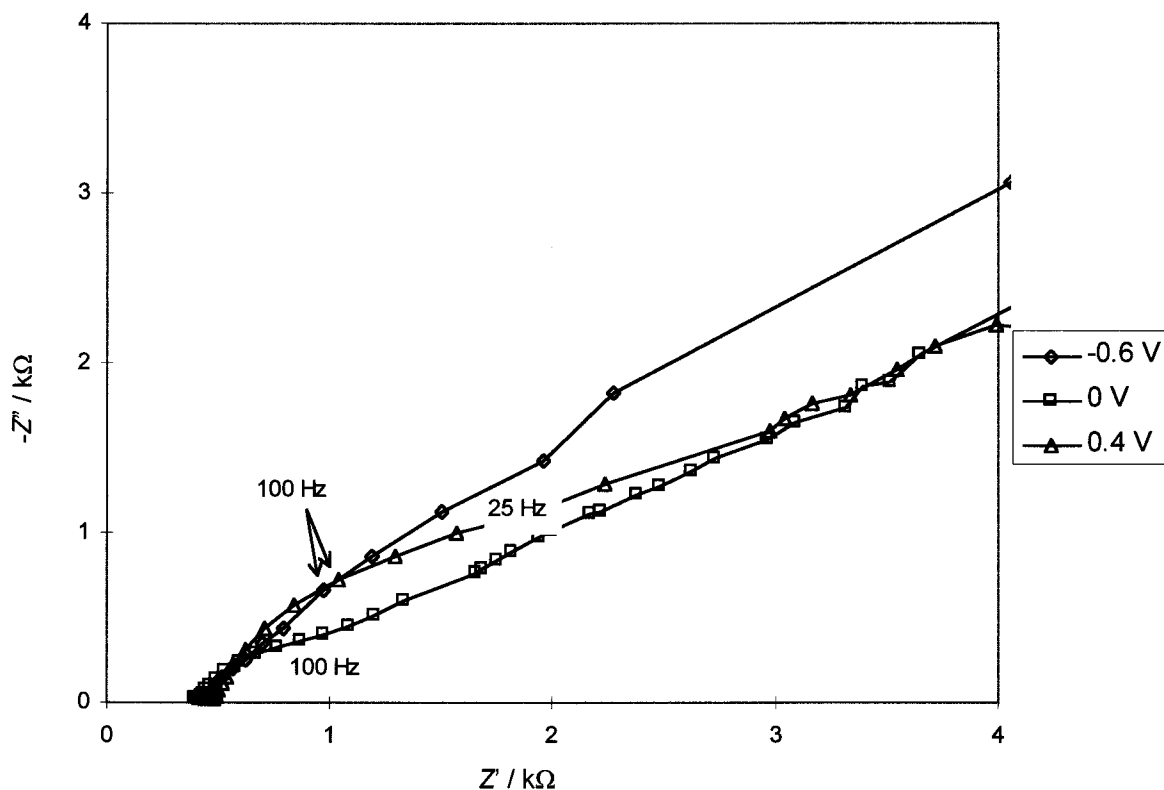
Fig. 10. Nyquist plots of overoxidized PPy–AHSA in PBS at − 0.6, 0 and 0.4 V.

due to Ab–Ag binding. These results are consistent with the proposed mechanism involving the interactions between the negatively charged Ab at a neutral pH, plus a delocalized positive charge along a CEP chain, and the adsorption of the antigen. It also explained the shifts in the anodic and cathodic waves from the CV experiments. The interaction induces a change in the capacitance of the polymer, resulting in the polarization of the electrode, and consequently the analytical signal. Both the CV and impedance experiments showed that this potential dependent shift could be attributed to Ab–Ag binding.

Acknowledgements

References

[1] G. Bidan, Sensors & Actuators B6 (1992) 45.
[2] O.A. Sadik, Anal. Methods and Instrumentation 2 (1995) 293.
[3] W. Schuman, Mikrochim Acta 121 (1995) 1.
[4] E.I. Iwuoha, D. Saentz de Villaverde, N.P. Garcia, M.R. Smyth, J.M. Pingarron, Biosensors and Bioelectronics 12 (1997) 749.
[5] O. Sadik, G. Wallace, Anal. Chim Acta 279 (1993) 209.
[6] O. Sadik, M. John, G. Wallace, D. Barnett, D. Laing, D. Clarke, Analyst 119 (1994) 1997.
[7] D. Barnett, D.G Laing, S. Skopec, O.A. Sadik, G.G. Wallace, Anal. Lett. 27 (1994) 2417.
[8] O.A. Sadik, J.M. Van Emon, Chem. Tech. 27 (1997) 38.
[9] O.A.Sadik,J.M Van Emon,Biosensor and Bioelectronics 11(1996)1.
[10] A. Sargent, O.A. Sadik, Anal. Chim. Acta 376 (1998) 125.
[11] K. Nirova, S. Bazovoski, Synthetic Metals 76 (1996) 229.
[12] S. Roth, H. Vbleier, Adv. Phys. 36 (1987) 385.
[13] J. Lippe, R. Holze, Syn. Metals. 41–43 (1991) 2927.
[14] M.E.G. Lyons, C. Lyons, C. Fitzgerald, T. Bannon, Analyst 118 (1993) 361.
[15] O.A. Sadik, G.G. Wallace, Electroanalysis 5 (1993) 555.
[16] M.A. De Paoli, R.C.D. Peres, S. Panero, B. Scrosatti, Electrochim. Acta 37 (1992) 419.
[17] X. Ren, P.G. Pickup, J. Phys. Chem. 97 (1993) 5356.
[18] A. Haimerl, A. Mertz, J. Electroanal. Chem 220 (1987) 445.
[19] A. Sibai, K. Elamri, D. Barbier, N. Jafferzic-Renault, E. Souteyrand, Sensors and Actuators B31 (1996) 125.
[20] P.R. Mathewson, J.W. Finley (Eds.), Biosensor Design and Application, ACS Symposium Series 511, American Symposium Society, Washington, DC, 1992, p. 89.
[21] T. Koboyashi, H. Yoneyama, H. Tamura, J. Electroanal. Chem. 177 (1984) 281.
[22] R. Bull, F. Fan, A. Bard, J. Electrochem. Soc. 129 (1982) 1009.
[23] S. Felberg, J. Am. Chem. Soc. 106 (1984) 4671.
[24] N. Marmillod, J. Tanguy, F. Petiot, J. Electrochem. Soc. 133 (1986) 1073.
[25] J. Tanguy, N. Marmillod, M. Hoclet, J. Electrochem. Soc. 134 (1987) 795.
[26] S.N. Hoier, D.S. Ginye, S. Park, J. Electrochem. Soc. 135 (1988) 91.
[27] P. Daun, R. Murray, J. Electrochem. Soc. 103 (1979) 289.
[28] J. Mostany, B.R. Scharifker, Synth. Met. 87 (1997) 179.
[29] P. Bataillard, F. Gardies, N. Jaffrezic-Renault, C. Martelet, Anal. Chem. 60 (1988) 2374.
[30] F. Gardies, C. Martellet, Sensors and Actuators 17 (1989) 461.